RETARDATION OF FATIGUE CRACK GROWTH BY A SINGLE OVERLOAD

J.N. EASTABROOK*

An approximate calculation is made of the way in which the residual stresses due to a single overload affect the subsequent growth of a fatigue crack growing under constant-amplitude loading in plane-strain conditions. The calculation is free of arbitrary parameters and describes the effect in terms of a residual stress intensity factor which depends on the stress intensity factor of the overload and on the crack growth since the overload occurred. It accounts for the variations of growth rate observed in published experiments, including the phenomenon of delayed retardation.

INTRODUCTION

In the design of damage-tolerant aircraft structures, small cracks are postulated to exist in various parts of the structure and their growth by fatigue during service is predicted using laboratory data. Aircraft service loads cause irregular fluctuations of stress, and the statistical parameters describing these fluctuations depend on the type of aircraft, the type of service and the part concerned. It is uneconomic to perform flight-simulation fatigue tests using stress sequences representing every case, and at present the crack growth is often predicted from constant-amplitude data by assuming that the growth during each cycle is the same as in constant-amplitude fatigue.

This assumption has often been found to give unduly conservative results, but no reliance can be placed on this apparent safety factor, because it does not always exist. Reliable methods of predicting crack growth in the presence of these so-called "load interaction effects" are therefore being sought. One approach is to attempt to identify some of the important phenomena by experiments using very simply load sequences. A sequence demonstrating the major effect, which is *crack growth retardation* following an overload, is shown in Fig 1a, and its effect on crack growth is sketched in Fig 1b.

Many physical phenomena have been considered as causing or influencing this behaviour (1). At present most attention is paid to crack closure (2,3) and residual stress (4,5,6). Some empirical methods of predicting crack growth have been based on the residual stress concept, but it remains an open question whether the residual stresses which are likely to be present could produce the observed retardation. A simple model has therefore been set up, allowing a calculation of the effect of residual stresses to be made by the methods of linear elastic fracture mechanics,

*Royal Aircraft Establishment, Farnborough, Hants, UK

for a single overload in a constant-amplitude sequence under plane-strain conditions.

Published experiments for this case show that as the crack tip grows away from the point of overload the crack rate falls rapidly, but not immediately, to a minimum and then slowly returns to normal. The present calculation which, though approximate, contains no arbitrary constants, reproduces this behaviour and accounts for both the magnitude and the duration of the reduction in growth rate. This strongly suggests that residual stress is the most important factor in the case considered, and hence probably also in the general case. If so, a generalization of the present calculation may improve the prediction of fatigue crack growth in aircraft.

THE EFFECT OF A PREVIOUS TENSILE LOAD ON CONDITIONS AT THE TIP OF A GROWING CRACK

We will assume that a body consisting of homogeneous isotropic material contains a planar crack and is subjected to stress such that the material surrounding the tip of the crack is in a state of plane strain, the mode II and mode III stress intensity factors are zero, and the mode I stress intensity factor K_I is gradually increased from zero. Plastic shear occurs immediately at the tip of the crack, because of the stress concentration, and the volume of the zone of plastically-sheared material increases as K_I increases. Because of the assumption of plane strain, it is only necessary to consider a section through the body perpendicular to the line of the crack tip (Fig 2). The size and shape of the plastic zone for any particular value of K_I depend on the yield stress of the material and its strain-hardening properties, but even for a non-strain-hardening material they are not well established. However, there is general agreement that the shape is something like that shown in Fig 2, with rather small extension in the plane of the crack. Various numerical analyses have found the lobes to be tilted either forward or backward by up to 20° from the position shown. The magnitude $\rho(\theta)$ of the radius vector from the tip of the crack to the boundary of the plastic zone, at any angle θ, is given approximately by

$$\rho(\theta) = Cf(\theta)\left(\frac{K_I}{\tau_f}\right)^2 \qquad (1)$$

where C is a constant, $f(\theta)$ is a function of θ defining the shape of the plastic zone and τ_f is the flow stress in shear.

If K_I is slowly reduced after reaching a value K_{max}, reverse plastic flow begins almost immediately at the crack tip, and the size of the zone of material which is being plastically deformed in the reverse direction increases as K_I is reduced. By the time K_I reaches zero, the linear dimensions of the reverse plastic zone are calculated to be about a quarter of the forward plastic zone (7). The material of the reverse plastic zone is all on the point of flowing, and hence must contain residual strains appropriate to shear stresses comparable with the flow stress in shear τ_f. The rest of the forward plastic zone has not experienced reverse plastic flow and hence also contains residual strains with

accompanying residual stresses. The residual strains persist during any subsequent crack growth, and should be taken into account, along with the applied stress or displacements, in any calculation of the stress intensity factor of the longer crack. These strains are accompanied by residual stresses which extend, in principle, through the whole body. It would be quite wrong to suppose that they have no effect when the crack tip has grown out of the original plastic zone; though it should be expected, in conformity with Saint-Venant's principle, that the effect will be small once the crack growth exceeds the linear dimensions of the forward plastic zone.

As there is no generally agreed solution for the residual strains in the plastic zone, and as the accurate evaluation of the effect of such strains on the stress intensity factor would be a formidable task, a simple model will be used to assess their effect on the subsequent behaviour of the crack. It is required to estimate the contribution of the residual strains to the stress intensity factor (assuming that the external load is such as to prevent contact between the faces of the crack), when the crack tip has advanced a distance a beyond the point at which K_{max} was applied and removed.

The forces exerted *by* the material of the plastic zone *on* the rest of the body because of the presence of residual strains are taken to act at the same value of y but at the plane $x = 0$ (Fig 2), rather than at the elastic-plastic interface. In other words, the plastic zone is replaced by a slit of equal height at $x = 0$, and the stresses which it exerted on the surrounding elastic material are represented by surface tractions on the two faces of the slit. The shear stresses are taken to be τ_f, over the height of the reverse plastic zone, falling to zero at the height of the forward plastic zone. The latter is, from equation (1),

$$y_{max} = Cf\left(\frac{\pi}{2}\right)\left(\frac{K_{max}}{\tau_f}\right)^2 = B\left(\frac{K_{max}}{\tau_f}\right)^2 \qquad (2)$$

where B is a dimensionless constant. Calculated plastic-zone sizes vary widely, but a range of B from 0.03 to 0.04 covers several recent calculations (12). Although the residual normal forces seem likely to be smaller, no quantitative information is available and their effects will not be considered further: the contribution of the shear forces will be assessed independently, bearing in mind that the normal forces may also be significant. The elastic problem to be solved is thus that of the curiously-shaped body shown in Fig 3, subjected to the stresses indicated. The shear stresses on the front face of the slit tend to reduce the stress intensity factor; those on the back face to increase it.

It is proposed to approximate this configuration by that shown in Fig 4, in which the slit representing the plastic zone is extended to infinity and the stresses on the back face of the slit are represented either

(a) by a point force at y_{max} equal to the integral of the stress over the back face (curve a), or

(b) by a mirror image of the real stress distribution about the point y_{max} (curve b).

It is hoped these models might bound the real case.

The stress intensity factor can now be calculated using the results of Rooke and Jones (8). For a tangential force Q applied at y, they give

$$K_I = \frac{Q}{\sqrt{\pi a}} P(\xi) \tag{3}$$

where $$P(\xi) = (1 - \xi^2)(1.2943 + 0.0044\xi + 0.1289\xi^2 + 10.89\xi^3 - 22.14\xi^4 + 10.96\xi^5) \tag{4}$$

and

$$\xi = \frac{y}{y + a} . \tag{5}$$

For a distribution of shear stress, $\tau(y)$, symmetrical about the crack plane, the stress intensity factor becomes

$$K_I = \frac{2}{\sqrt{\pi a}} \int_0^\infty \tau(y) P(\xi) dy \tag{6}$$

Let

$$\left.\begin{aligned} Y &= \frac{y}{y_{max}} \\ A &= \frac{a}{y_{max}} \\ T(Y) &= \frac{\tau(y)}{\tau_f} \end{aligned}\right\} \tag{7}$$

Then

$$\xi = \frac{Y}{Y + A}$$

and

$$K_I = \frac{2}{\sqrt{\pi a}} \int_0^\infty \tau_f T(Y) P(\xi) y_{max} dY \tag{8}$$

which becomes, using equation (2),

$$\frac{1}{\sqrt{B}} \left(\frac{K_I}{K_{max}}\right) = \frac{2}{\sqrt{\pi A}} \int_0^\infty T(Y) P'\left(\frac{Y}{A}\right) dY = \phi(A) \tag{9}$$

where P' is the function obtained from equations (4) and (5), and ϕ is a function of A alone.

The contribution of the front face to the integral in equation (9) is

$$\int_0^1 T(Y) P'\left(\frac{Y}{A}\right) dY$$

The shear stress on the back face is the reverse of that on the front face, so its contribution is, for model (a)

$$- P'\left(\frac{1}{A}\right) \int_0^1 T(Y) dY$$

where $P'(1/A)$ is the value of P' when Y is 1; and for model (b)

$$- \int_1^2 T(2 - Y) P'\left(\frac{Y}{A}\right) dY$$

The residual opening-mode stress intensity factor K_{res} for the shear stresses is therefore given by

$$\frac{K_{res}}{K_{max}\sqrt{B}} = \phi(A) \tag{10}$$

where for model (a)

$$\phi(A) = \phi_a(A) = \frac{2}{\sqrt{\pi A}} \left(\int_0^1 T(Y) P'\left(\frac{Y}{A}\right) dY - P'\left(\frac{1}{A}\right) \int_0^1 T(Y) dY \right) \tag{10a}$$

and for model (b)

$$\phi(A) = \phi_b(A) = \frac{2}{\sqrt{\pi A}} \left(\int_0^1 T(Y) P'\left(\frac{Y}{A}\right) dY - \int_1^2 T(2 - Y) P'\left(\frac{Y}{A}\right) dY \right) . \tag{10b}$$

The two expressions have been evaluated for the stress distribution shown in Fig 4, which is

$$\left.\begin{aligned} T &= -1 && 0 < Y < \tfrac{1}{4} \\ T &= -\tfrac{4}{3}(1 - Y) && \tfrac{1}{4} < Y < 1 \end{aligned}\right\} \qquad (11)$$

(the negative signs indicate that the forces are towards the crack). The results are shown in Fig 5. K_{res} is negative and thus tends to close the crack except at high values of A where a small positive value is calculated. The most negative values are of order $K_{max}\sqrt{B}$ and are within 12% of each other for the two models, but the effect persists about 50% longer for model (b). The results are not very sensitive to the way in which T varies with Y : in the extreme case where T is put equal to -1 over the whole range of Y from 0 to 1 , the negative peak of K_{res} is increased by about 10% and the effect persists 10-20% further.

APPLICATION TO CRACK GROWTH AFTER A SINGLE OVERLOAD

Suppose now that the crack growth following the application and removal of K_{max} is by fatigue under constant-amplitude loading as in Fig 1a, such that the minimum stress is zero (so the stress ratio R is also zero) and the peak stress intensity factor K_p is significantly less than K_{max} .

The following provisional conclusions may be drawn from Fig 5. Very little crack growth can occur if K_p/K_{max} is less than $\sqrt{B}$, because the residual stress will, in that case, not allow the crack to open once the crack growth a is about 1% of the plastic-zone height y_{max} . At slightly higher values of K_p , the crack may grow a small fraction of y_{max} before stopping. Continued crack growth occurs only if K_p is greater than about $1.25K_{max}\sqrt{B}$. If B has the value 0.04, for example, the crack will shortly cease to grow if K_p is less than about $0.25K_{max}$. At higher values of K_p , the crack will start to grow as if there had been no overload, but will rapidly slow down, passing through a minimum growth rate when a/y_{max} is about 0.08 and thereafter gradually accelerating, to reach nearly normal rates after growing a distance approximately equal to the height of the plastic zone. Note that the model 'predicts' crack closure.

This behaviour agrees qualitatively with the observed behaviour of a crack growing under constant-amplitude fatigue loading and subjected to a tensile overload during a single cycle (see Fig 1). Fig 5 could be used, along with data on crack growth at constant amplitude, to estimate crack growth rates after the single overload of Fig 1, by adding K_{res} to the applied maximum and minimum values (K_p and zero).

However, before a numerical comparison is attempted, it must be noted that each normal loading cycle also produces a plastic zone at the tip of the crack. This raises two important considerations: firstly, linear elastic fracture mechanics is usually considered to be strictly valid only if the plastic zone at the crack tip is small compared with the region in

which the stress field in an elastic body would be adequately represented by an expression of the form

$$kf(\theta)/\sqrt{2\pi r}$$

where r and θ are polar co-ordinates from the crack tip; secondly, the plastic zone of each normal cycle affects the value of K_{res} for subsequent cycles.

The first consideration will not affect the conclusions relating to crack arrest, since the size of the plastic zone at the tip of the crack would then be zero; nor would it affect the calculation of growth rate when K_p is only a little greater than $-K_{res}$, since then the plastic zone size $B(K_p + K_{res})^2/\tau_f^2$ will be small; but K_p will often be such that the plastic zone height is more than a , and then the validity of expressions based on linear elastic fracture mechanics is not assured. However, as discussed later, the error may turn out to be acceptable even in this case.

As to the second consideration, some allowance for the effect of previous normal cycles is easily incorporated if the calculation of growth rate is to be made, as previously suggested, by use of measurements of growth rate at constant amplitude. Then the effect of the overload is simply to substitute one overload cycle for one normal cycle (shown dotted in Fig 1a). This suggests that if K_{resp} is the residual stress intensity factor due to one normal cycle, the maximum and minimum values of K should be shifted, not by K_{res} , but by an amount K_s , where

$$K_s = K_{res} - K_{resp} \qquad (12)$$

and K_{resp} is the value of K_{res} obtained by substituting K_p for K_{max} in equations (2), (9) and (10). Then the effective values of the minimum and maximum K are K_s and $K_p + K_s$, so that the crack growth could be obtained from the usual constant-amplitude curves using

$$\Delta K_{eff} = K_p$$

and

$$R_{eff} = \frac{K_s}{K_p + K_s} \qquad (13)$$

Note that this calls for constant-amplitude curves at negative R .

Some error may remain after this correction because it does not allow for interactions with other cycles of the constant-amplitude sequence. It might be possible to take these multiple secondary effects into account, but for this first discussion they will be disregarded.

Equation (12) can be written, using equation (10)

$$\frac{K_s}{\sqrt{B}} = K_{max}\phi\left(\frac{a}{y_{max}}\right) - K_p\phi\left(\frac{a}{y_p}\right) \qquad (14)$$

where y_p is the size of the plastic zone produced by K_p (as in equation (2)). This equation should be valid when K_p is small compared with K_{max}, as discussed in the last paragraph but two. It also holds when K_{max} is equal to K_p (*ie* no overload) because then the correction is zero, as it should be. Therefore it may well be a tolerable approximation for intermediate values, in spite of the problem with the validity of linear elastic fracture mechanics. For computation, equation (14) can be written in the alternative form

$$\frac{1}{\sqrt{B}}\left(\frac{K_s}{K_p}\right) = \beta\phi(A) - \phi(\beta^2 A) \qquad (15)$$

where β is the overload ratio K_{max}/K_p. The results are shown in Fig 6 for approximation (a).

Crack arrest will occur if $K_p + K_s$ is less than K_T, the threshold value for crack growth, that is if

$$\frac{K_p}{K_T} < \left(1 + \frac{K_s}{K_p}\right)^{-1} \qquad (16)$$

For a given value of β, continued crack growth will therefore occur only if

$$\frac{K_p}{K_T} > \left[1 + \left(\frac{K_s}{K_p}\right)_{min}\right]^{-1} \qquad (17)$$

where $(K_s/K_p)_{min}$ is the minimum of the appropriate curve in Fig 6. Let the corresponding value of A be A_{min}. If K_p is too small to meet the condition (17), crack arrest will occur at some value of A less than A_{min}. Fig 7, derived from relation (17) and equation (15) or Fig 6, shows the predicted boundary between continued crack growth and crack arrest as a function of K_p/K_T and the overload ratio β, for B equal to 0.04.

COMPARISON OF PREDICTED RETARDATION WITH PUBLISHED EXPERIMENTAL RESULTS

Many of the published measurements were made under plane stress conditions and are therefore not suitable for comparison with the present plane strain calculation. In other work, the crack advance after overload was measured at the surface of the sheet or plate with a travelling microscope. Robin

and Pelloux (9) have demonstrated by counting striations that the crack retardation after multiple overload is greater at the surface of a 12.7 mm plate of 2124-T351 aluminium alloy than in the middle, and no doubt the same is true for a single overload: thus surface measurements probably over-estimate the crack retardation under plane strain conditions.

Wei *et al* (10) have used an electrical method, which averages crack growth along the crack front, for measurements on 2219-T851 aluminium alloy 16.5 mm thick at a stress ratio R of 0.05 and an overload ratio of 2.0. Constant-amplitude measurements, made by the same group (11), are available for the same alloy 12.7 mm thick, but not for the negative stress ratios needed for the method of calculation suggested above. To make some comparison, the common approximation that compressive applied stresses have no effect during constant-amplitude fatigue crack growth has therefore been used. The constant-amplitude data was extrapolated slightly to cover the range from R = 0.05 to R = 0, and was used with effective values of ΔK and R defined by

$$\left.\begin{aligned} \Delta K_{eff} &= \Delta K \\ R_{eff} &= \frac{0.05K_p + K_s}{K_p + K_s} \end{aligned}\right\} 0.05K_p + K_s \geqslant 0$$

$$\left.\begin{aligned} \Delta K_{eff} &= K_p + K_s \\ R_{eff} &= 0 \end{aligned}\right\} 0.05K_p + K_s < 0 \qquad (18)$$

to calculate the ratio of the crack growth rate after overload to the rate before overload.

In Fig 8 the shaded area is the scatter band of Wei *et al*, and the curves are calculated for B = 0.03 and 0.04, which encompass the range of recent numerical calculations (Ref 12, Table 1), and for models (a) and (b). The curve for B = 0.03, model (b), lies quite close to that for B = 0.04, model (a), and has been omitted for clarity. The general way in which the growth rate depends on the distance the crack tip has moved since the overload is well described by the calculation, and the magnitude of the reduction is roughly equal to that observed.

The centre-section measurements (9) for an overload ratio of 1.3 would be suitable for comparison with the present plane-strain calculation, except that they were made after the application of two successive overloads. The comparison is nevertheless made in Fig 9. The value of τ_f was estimated from data in Ref 9, but as constant-amplitude data for the 2124 alloy were not to hand, the data for 2219 alloy was used, as before, to estimate the crack advance for given values of ΔK_{eff} and R_{eff}. (It is not thought that the substitution will cause much error, because the calculation is concerned only with the ratios of crack rates, rather than with absolute values.) The difference between the calculated and measured curves is similar to that between the surface measurements for one and two overloads (13).

DISCUSSION

Although several sweeping assumptions were made in the course of the analysis, the calculated retardation agrees qualitatively with the results of a number of experiments and quantitatively with one or two cases where a numerical comparison was feasible. In particular, the calculation gives a rational explanation of the phenomenon of delayed retardation.

The assumption that the crack tip is growing through material which has not been deformed by the overload is false for small crack extensions. The high deformation of the material just in front of the crack tip at overload may be the reason for the crack acceleration which has sometimes been observed for a very short distance following an overload, since prior deformation can increase crack growth rate (14,15). However, the effect on a prediction of total crack growth would seem to be very small, since the acceleration occurs over such a short distance.

The model gives a straightforward qualitative explanation for the increase of crack opening stress after an overload, but does not require any measurement of crack closure. For the case considered, in the absence of general plasticity, the effect of an overload can be described in terms of a residual stress intensity factor which is calculated from the flow stress and the overload stress intensity factor in the way shown.

An extension of the analysis to positive and negative R values and to multiple overloads would be highly desirable, to provide a sound basis for a general method of predicting crack growth under variable-amplitude loading. It appears that any extension would need to take account of the effect of zone overlap due to the finite size of the plastic zones in the x direction.

CONCLUSIONS

The major effects of a single overload on subsequent fatigue crack growth under plane-strain conditions can be described in terms of a residual stress intensity factor associated with the stresses which the material of the overload plastic zone exerts on the surrounding undeformed material. An approximate calculation of the effect on subsequent crack growth of this residual stress intensity factor agrees with limited experimental information.

LIST OF SYMBOLS

a	crack extension beyond point of overload
A	a/y_{max}
B	dimensionless constant
C	a constant
K_I	mode I stress intensity factor (SIF)
K_{max}	maximum value of K_I

LIST OF SYMBOLS (concluded)

K_p	peak SIF of the constant-amplitude sequence
K_{res}	residual opening-mode SIF due to K_{max}
K_{resp}	residual opening-mode SIF due to K_p
K_s	$K_{res} - K_{resp}$
K_T	threshold SIF for fatigue crack growth ($R = 0$)
ΔK	twice the amplitude of SIF in a fatigue cycle
ΔK_{eff}	effective value of ΔK to account for residual stress
P, P'	defined functions of y and a
r	radial polar coordinate from the crack tip
R	stress ratio of fatigue cycle
R_{eff}	effective value of R to account for residual stress
T	τ/τ_f
x	cartesian co-ordinate
y	cartesian co-ordinate
y_{max}	height of plastic zone corresponding to K_{max}
y_p	height of plastic zone corresponding to K_p
Y	y/y_{max}
β	overload ratio K_{max}/K_p
θ	angular polar co-ordinate from the crack tip
ξ	dimensionless variable $y/(y + a)$
$\rho(\theta)$	radius of plastic zone in direction θ
τ	shear stress
τ_f	flow stress in shear
$\phi(A)$	a function of A alone

REFERENCES

1 Schijve, J., Department of Aeronautical Engineering Report VTH-18 (Delft University of Technology, Netherlands, 1974).

2 Elber, W., in "Damage tolerance in aircraft structures ASTM STP 486", 230, (American Society for Testing Materials, 1971).

3 Newman, J.C., in "Design of fatigue and fracture resistant structures ASTM STP 761", 255, (American Society for Testing Materials, 1982).

4 Wheeler, O.E., J. Bas. Eng., 94, (1972) 181.

5 Willenborg, J.D., Engle, R.M., and Wood, H.A., AFFDL-TM-FBR-71-1, (Air Force Flight Dynamics Laboratory, USA, 1971).

6 Johnson, W.S., in "Methods and models for predicting fatigue crack growth under random loading, ASTM STP 748", 85, (American Society for Testing Materials, 1981).

7 Rice, J.R., in "Fatigue crack propagation, ASTM STP 415", 247 (American Society for Testing Materials, 1967).

8 Rooke, D.P., and Jones, D.A., J. Strain Anal., 14, (1979) 1.

9 Robin, C., and Pelloux, R.M., Mater. Sci. and Eng., 44, (1980) 115.

10 Wei, R.P., Fenelli, N.E., Unangst, K.D., and Shih, T.T., J.Eng. Mater. Technol., 102 (1980) 280.

11 Unangst, K.D., Shih, T.T., and Wei, R.P., Eng. Fracture Mech., 9, (1977) 725.

12 Lankford, J., Davidson, D.L., and Cook, T.S., in "Cyclic stress-strain and plastic deformation aspects of fatigue crack growth, ASTM STP 637" 36, (American Society for Testing Materials, 1977).

13 Mills, W.J., Hertzberg, R.W., and Roberts, R., in "Cyclic stress-strain and plastic deformation aspects of fatigue crack growth, ASTM STP 637", 192, (American Society for Testing Materials, 1977).

14 Shijve, J., Eng. Fracture Mech., 8, (1976) 575.

15 McDarmaid, D.S., RAE TR 79148, (Royal Aircraft Establishment, 1979).

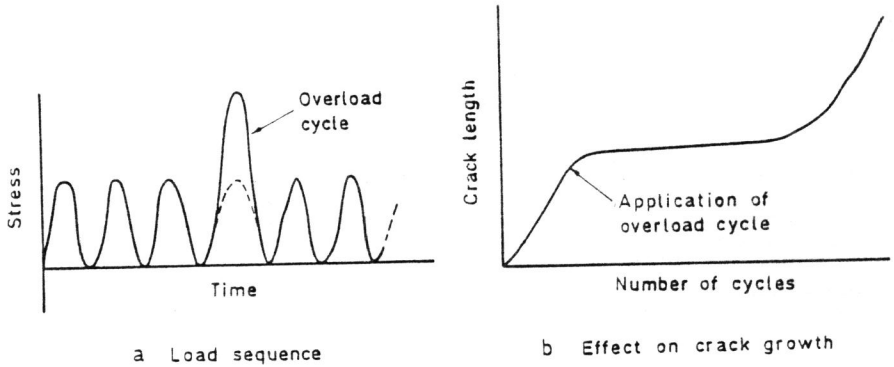

Fig 1a&b Effect of overload on fatigue crack growth

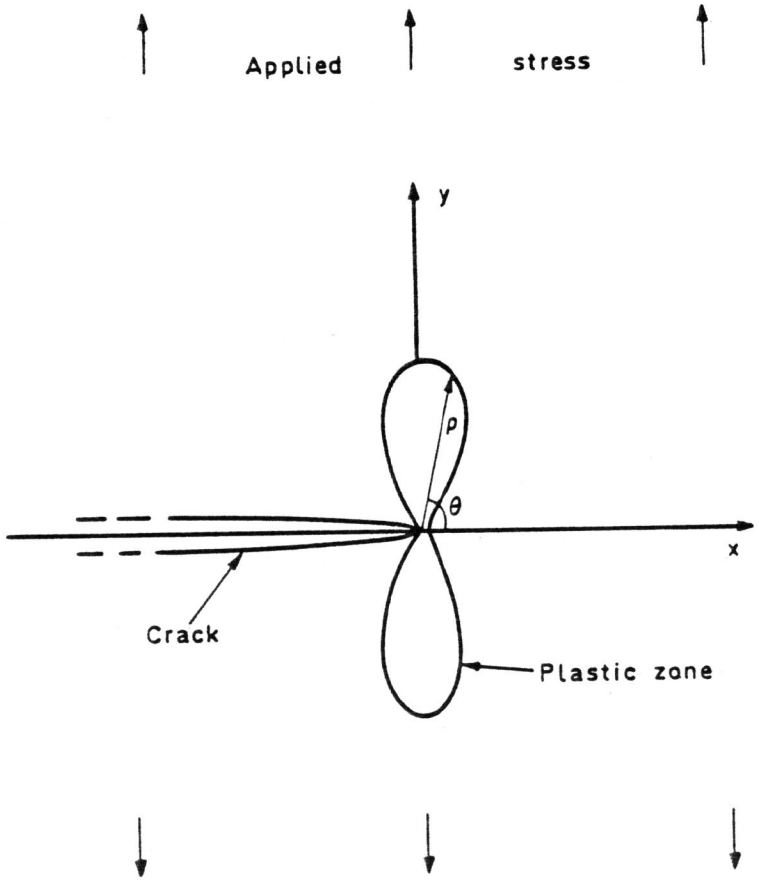

Fig 2 Approximate shape of plastic zone: mode 1, plane strain

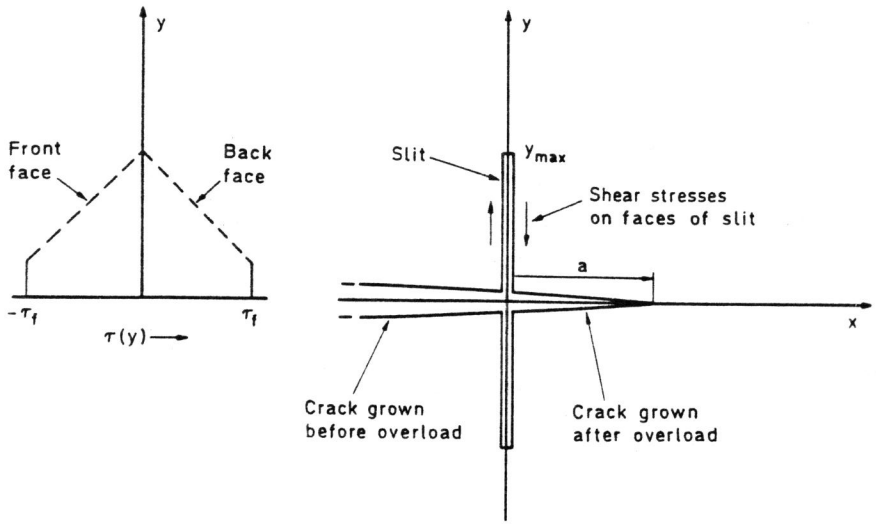

Fig 3 Plastic zone simulated by slit with shear stresses

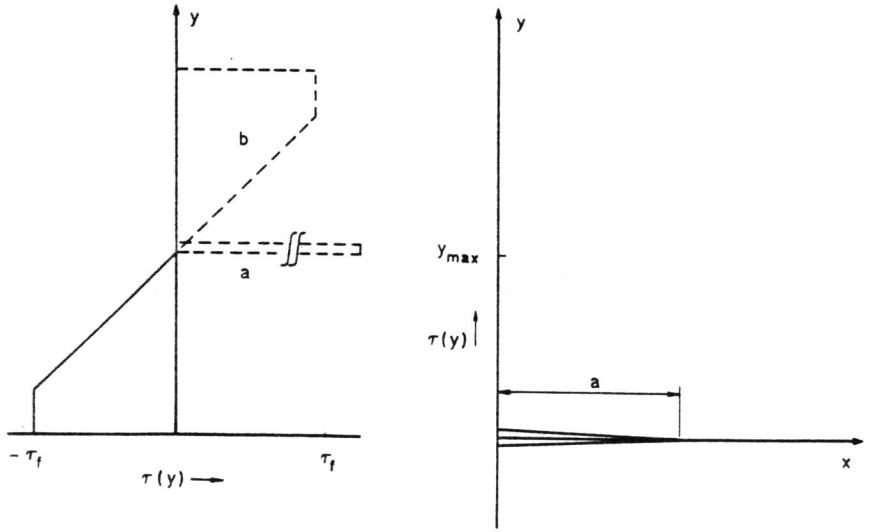

Fig 4 Further simplification of the elastic problem

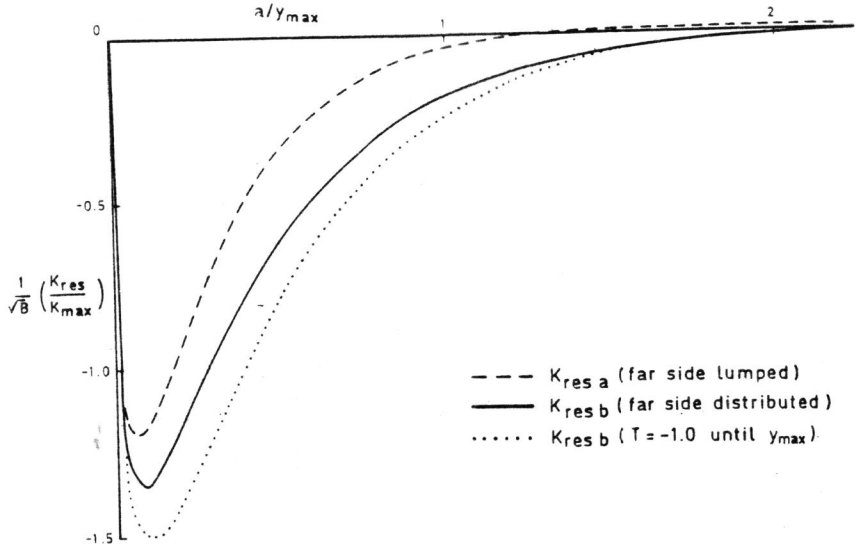

Fig 5 Dependence of residual stress intensity factor on crack extension: various approximations

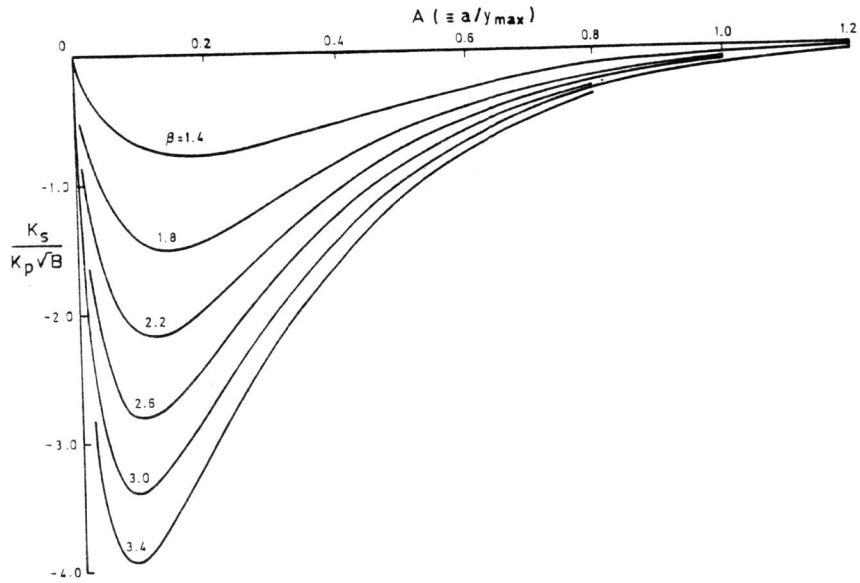

Fig 6 Estimated shift of the residual stress intensity factor due to a single overload, for various values of the overload ratio

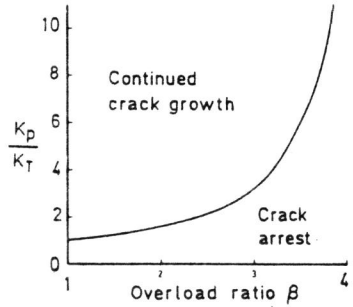

Fig 7 Conditions for crack arrest

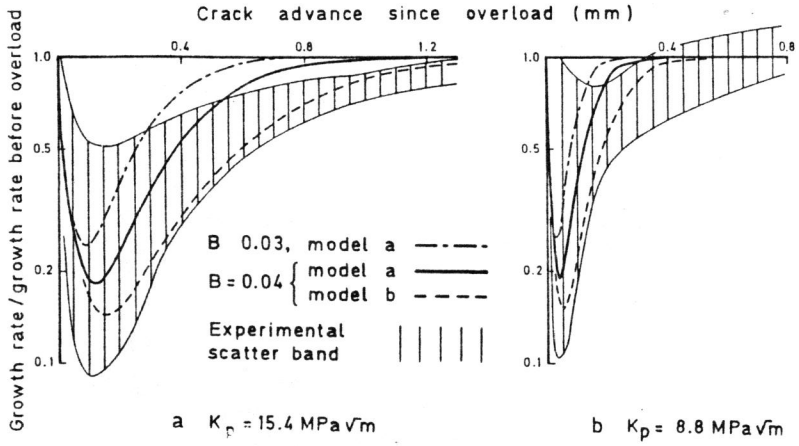

Fig 8a&b Calculated retardations compared with the experimental results of Wei *et al.* Overload ratio 2:1

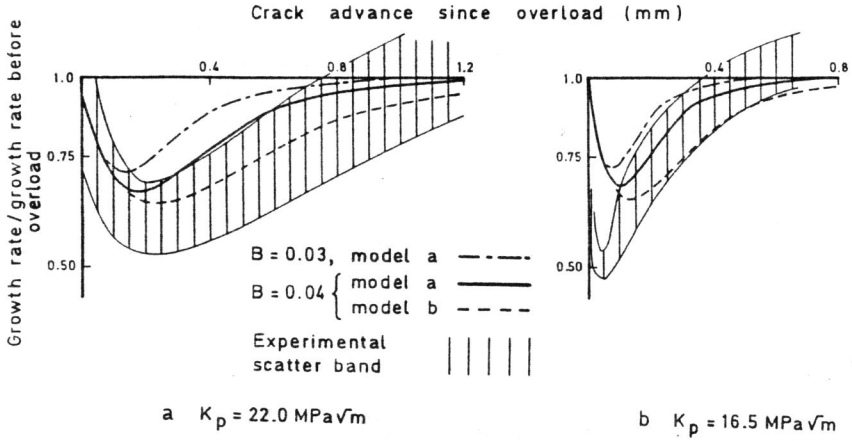

Fig 9a&b Calculated retardations for a single overload compared with the experimental results of Robin and Pelloux for a double overload. Overload ratio 1.3:1

Composição e impressão:
Oficinas Gráficas da Editorial do LNETI